SEISMIC STRUCTURE OF THE OCEAN CONTINENT BOUNDARY IN THE NEWFOUNDLAND BASIN FROM A MULTICHANNEL SEISMIC LINE

Jane Elizabeth Hawken

Submitted in partial Fulfillment of the Requirements
For the Degree of Bachelor of Science, Honours
Department of Earth Sciences
Dalhousie University, Halifax, Nova Scotia
March 20, 2003

Dalhousie University

Department of Earth Sciences
Halifax, Nova Scotia
Canada B3H 3J5
(902) 494-2358
FAX (902) 494-6889

DATE April 30, 2003

AUTHOR Jane Elizabeth Hawken

TITLE Seismic Structure of the Ocean Continent Boundary in the Newfoundland Basin from a multichannel seismic line

Degree B.Sc. Convocation May 20 Year 2003

Abstract

Detailed wide-angle Ocean Bottom Seismometer and vertical incidence multichannel seismic (MCS) data were collected along three main transects across the Newfoundland Shelf as part of the Study of Continental Rifting and Extension on the Eastern Canadian sHelf (SCREECH). Extending from continental to oceanic crust these lines were acquired to study structures formed during the Mesozoic rifting of the Grand Banks and Iberia margins. Line 306, an auxiliary MCS line parallel to the seaward portion of the southern most transect line 3mcs2, was processed. This processing sequence included common mid-point sorting, frequency filtering, and normal moveout corrections prior to stacking and post-stack finite difference migration. This processing confirmed the continuity of basement highs adjacent to oceanic crust on the seaward end of line 3MCS2. Results from processing show a single basement high in the ocean continent transition on line 306. These structures are interpreted as fault blocks which represent tectonic activity prior to the onset of seafloor spreading.

Table of Contents

List of Figures

Acknowledgements

I would like to thank Keith Louden for the opportunity to work on this project. I would also like to thank Pat Ryall for his feedback and for the use of his many books. This project would not have been possible without the help of Chris LeBlanc. He provided me with computer assistance and was always available to answer questions. Helen Lau was kind enough to allow me to use results from processing of line 3mcs2. Helen also gave her insight which helped me to interpret my line. And last but not least I would like to extend my deepest gratitude to Garth DeMont for the many times he proofread this thesis, making it what it is.

Chapter 1: Introduction

1.1 Background

The North Atlantic continental margin, formed by the Mesozoic rifting of Iberia and Africa from North America, is a typical example of a nonvolcanic rifted margin. Substantial extrusive basaltic volcanism or igneous underplating of the lower crust are not evident at nonvolcanic margins while volcanic margins are characterized by extensive extrusive and intrusive magmatism (Reid, 1994). A lack of large scale syn-rift volcanism at the North Atlantic continental margin preserves the extensional fabric formed during lithospheric extension (Louden and Chian, 1999), thus providing an important environment in which to collect data for detailed studies of the margin's rift to drift history.

The Study of Continental Rifting and Extension in the Eastern Canadian sHelf (SCREECH) project was undertaken in 2000, along a small section of the North Atlantic continental margin located off the coast of Newfoundland, Canada. Seismic line 306, processed for this study, was shot in the Newfoundland Basin as part of this larger project. The western portion of line 306 images the seaward extent of the ocean continent transition (OCT), a zone of uncertain crustal affinity, before crossing into oceanic crust.

1.2 Evolution of the Newfoundland Basin

The Newfoundland Basin is part of the passive continental margin located off the coast of Newfoundland. It is a deep water basin (~4500 m) bounded by the Flemish Cap to the north and the southeast Newfoundland Ridge to the south, Figure 1.2.1. The Newfoundland Seamounts, a series of circular bathemetric highs transect the centre of the basin.

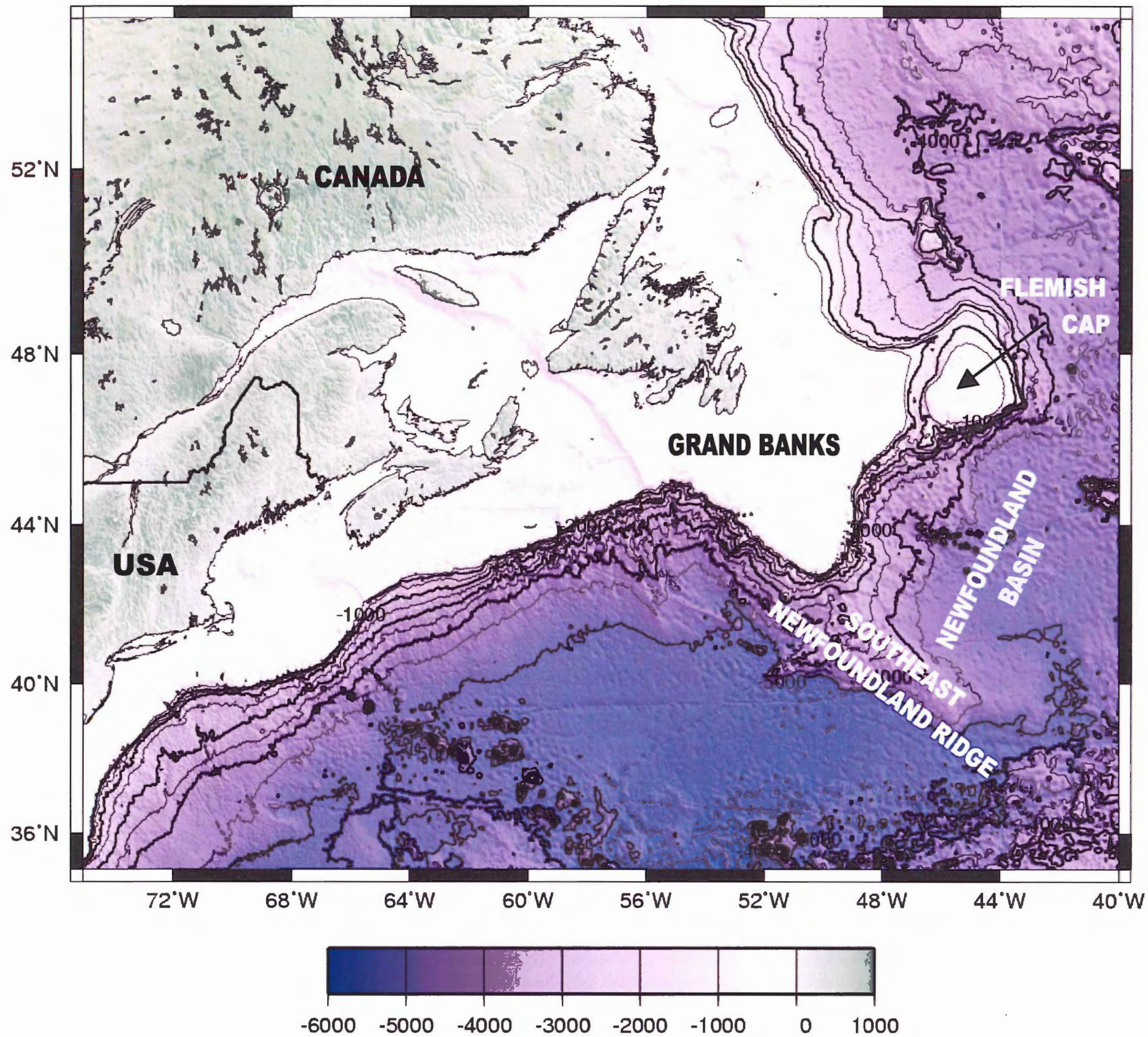

Figure 1.2.1 Location of Newfoundland Basin relative to the eastern Canada-USA boarder. The Newfoundland Basin is bounded by the Flemish Cap to the north, the Grand Banks to the west and the southeast Newfoundland Ridge to the south. Contours are in meters above sea level. Contour interval is every 500m with bold contours every 1000m.

The Newfoundland Basin marks the site of final rifting between Iberia and the Grand Banks in the mid-Cretaceous (Tucholke and Ludwig, 1982; Sullivan, 1983; Masson and Miles, 1984). This rifting was concentrated in two phases during the Mesozoic. The Southeast Newfoundland Ridge also known as the Newfoundland Fracture Zone is an anomalous physiographic feature that extends approximately 900 km southeast from the Grand Banks, (Grant and McAlpine, 1990). This ridge represents a transfer fault and the boundary between the two phases of rifting. The first phase of rifting between Africa and North America, south of the southeast Newfoundland Ridge, spanned 20 m.y. in the Late Triassic (Tucholke et al., 1989). The second rift phase between Newfoundland and Iberia, north of the southeast Newfoundland Ridge continued from the Late Triassic until Barremian-Aptian time (anomaly M1-M0) when the Grand Banks separated from Iberia (Tucholke and Ludwig, 1982; Sullivan, 1983).

The end of rifting and the onset of sea-floor spreading in the Newfoundland Basin are marked by a high-amplitude magnetic anomaly, called the J-anomaly, Figure 1.3.1. The J-anomaly formed by emplacement of anomalously thick or anomalously magnetized ocean crust between M0 and M1 time, corresponds to the Mesozoic sequence of oceanic spreading anomalies (Rabinowitz et al., 1978: Tucholke et al. 1989). This linear magnetic anomaly, which is observed on both sides of the North Atlantic Ocean, is generally coincident with a structural ridge or step in oceanic basement (Tucholke and Lugwig, 1982). A well defined, northeast trending linear topographic feature is associated with the J-anomaly south of the Southeast Newfoundland Ridge, Figure 1.3.1. The J anomaly is offset approximately 100 km southeast across the Southeast Newfoundland Ridge, and it progressively decreases in amplitude as it extends north into the Newfoundland Basin, particularly north of the Newfoundland seamounts.

Between the J-anomaly and anomaly 34, Figure 1.3.1, there are no magnetic spreading anomalies. This gap corresponds to the Cretaceous Quiet Period when there were essentially no magnetic reversals. The magnetic pattern between J-anomaly and anomaly 34 reflects magnetic variations in the basement.

Approximately 12 m.y. after the formation of the J-anomaly the spreading geometry in the Newfoundland Basin changed (Sullivan, 1978). The Newfoundland Seamounts, a chain of 13 seamounts lying in a triangular area near the center of the Newfoundland Basin, Figure 1.3.3, represent volcanic activity along faults formed by plate rotation associated with the change in spreading centers (Sullivan, 1978; Srivastava et al., 2000). Geochemical and petrological studies of dredged samples collected from three of the seamounts found alkali basalt and sodic trachyte compositions characteristic of oceanic volcanic rocks that occur on oceanic islands and at hot spots (Sullivan and Keen, 1977). Plagioclase grains of the trachytes from the three seamounts provide $^{40}Ar/^{39}Ar$ dates with an average Cretaceous age of 97.8 ±1.5 m.y. (Sullivan and Keen, 1977) some 10 to 20 m.y. younger than the oldest oceanic crust on which they reside (Tucholke et al., 1989).

1.3 Study Location

Multichannel seismic lines were acquired in the Newfoundland Basin as part of the Study of Continental Rifting and Extension on the Eastern Canadian sHelf (SCREECH). The survey had three main transects oriented NW-SE, perpendicular to the continental margin. Auxiliary lines were shot parallel and perpendicular to the main transects, Figure 1.3.2.

The southern most auxiliary line, line 306, is parallel to the oceanward portion of the most southern main transect line 3mcs2. Line 306 transects both the J-anomaly and the Scruncheon Seamount, Figures 1.3.1 and 1.3.3 respectively. In total approximately 3000 km of seismic line were recorded, encompassing continental crust on both the Flemish Cap and the Grand Banks, the assumed location of the OCT and a defined area of oceanic crust east of the J-anomaly in the Newfoundland Basin.

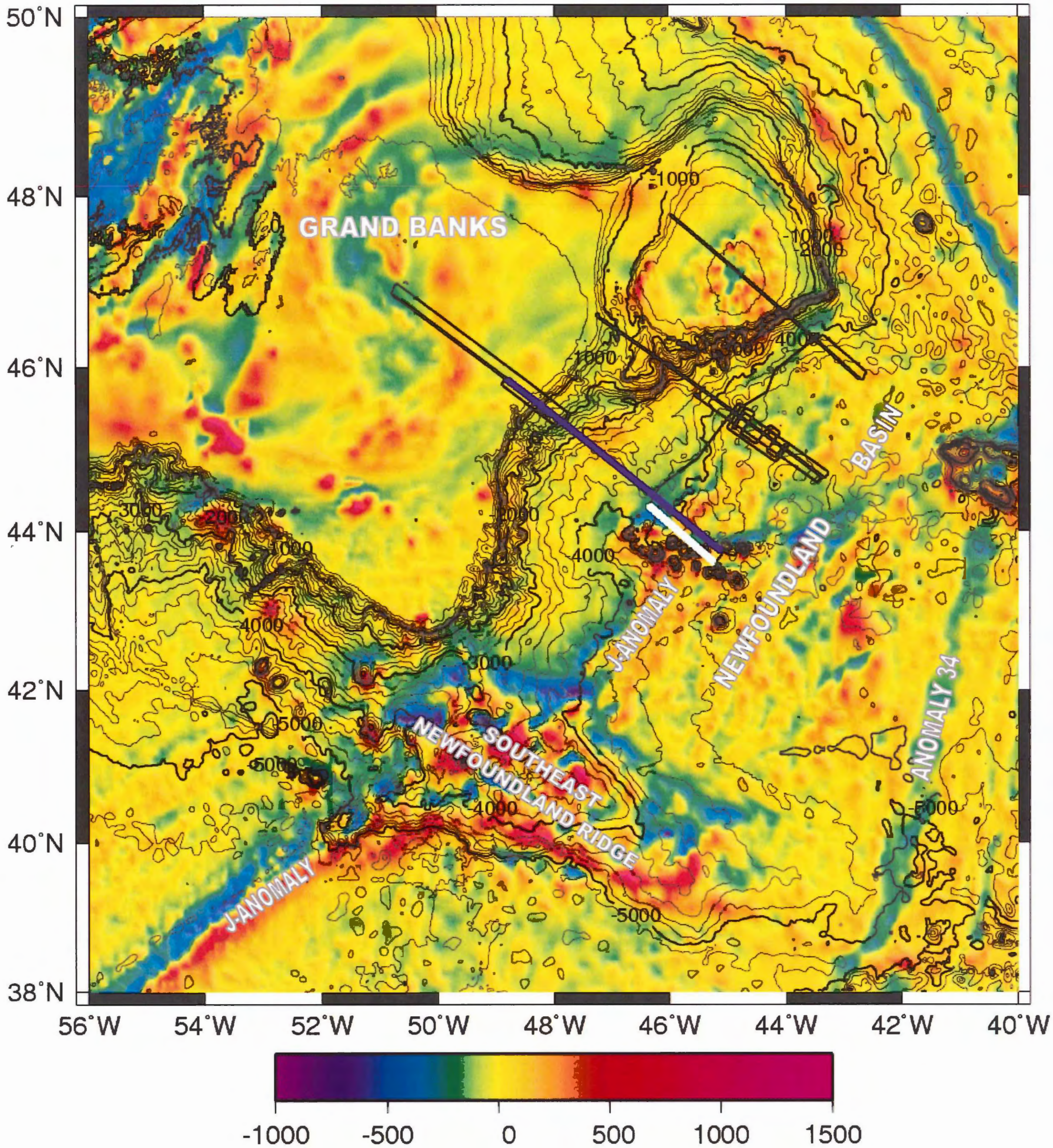

Figure 1.3.1 Magnetic map of the Newfoundland Basin. The J-anomaly is a strong and linear feature located south of the southeast Newfoundland Ridge but it weakens and breaks up north of the ridge. Magnetic colour contours in nT and bathemetric contours in meters above sea level. SCREECH seismic Line 306 in bold white, line 3mcs2 in bold blue and auxiliary lines in black.

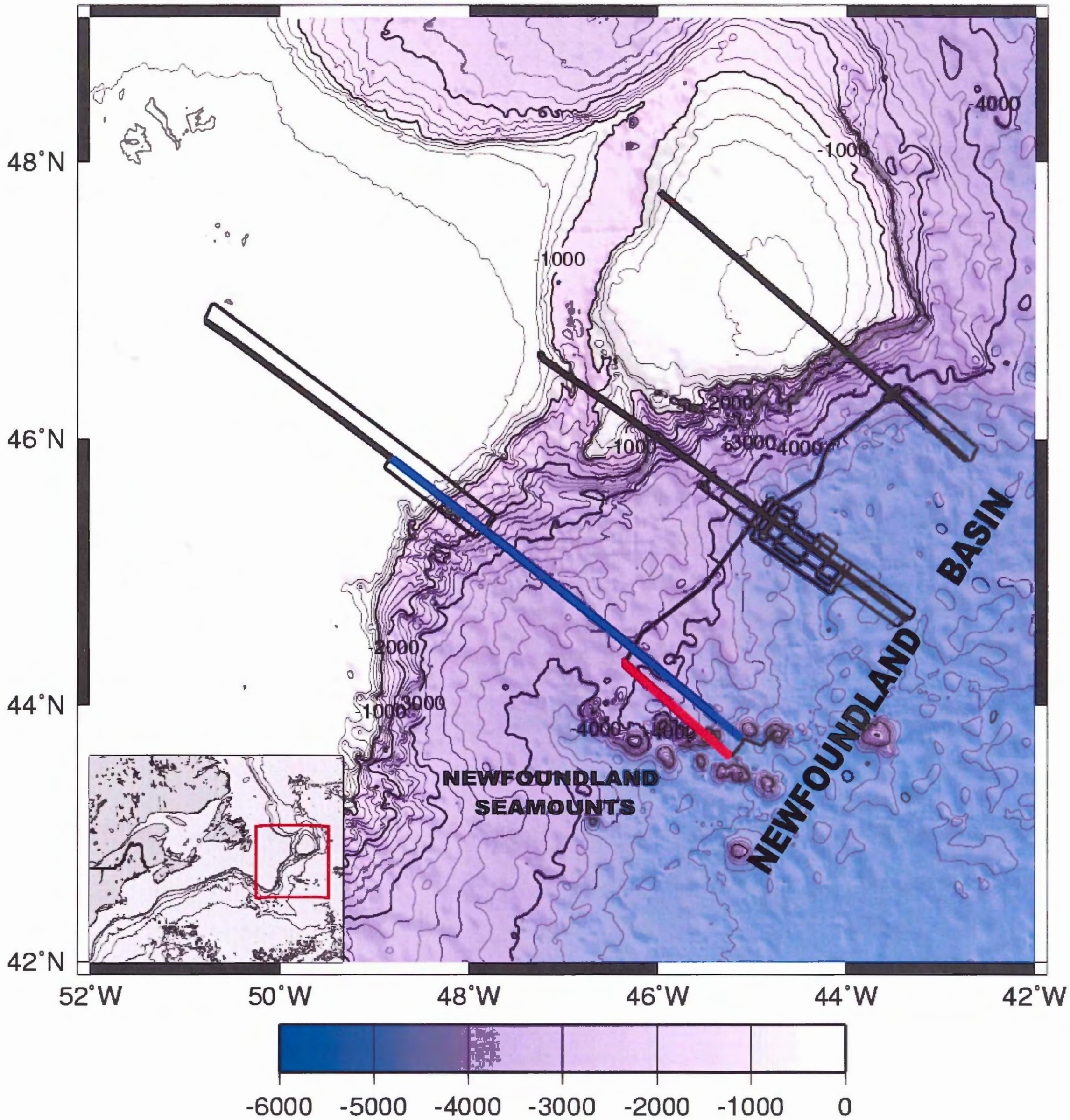

Figure 1.3.2 Detailed map of the location of the study area relative to Eastern Canada. Line 306 is in bold red and 3mcs2 in bold blue. Thick black lines are the 3 main seismic transects perpendicular to the margin. Thin black lines represent auxiliary multichannel seismic lines.

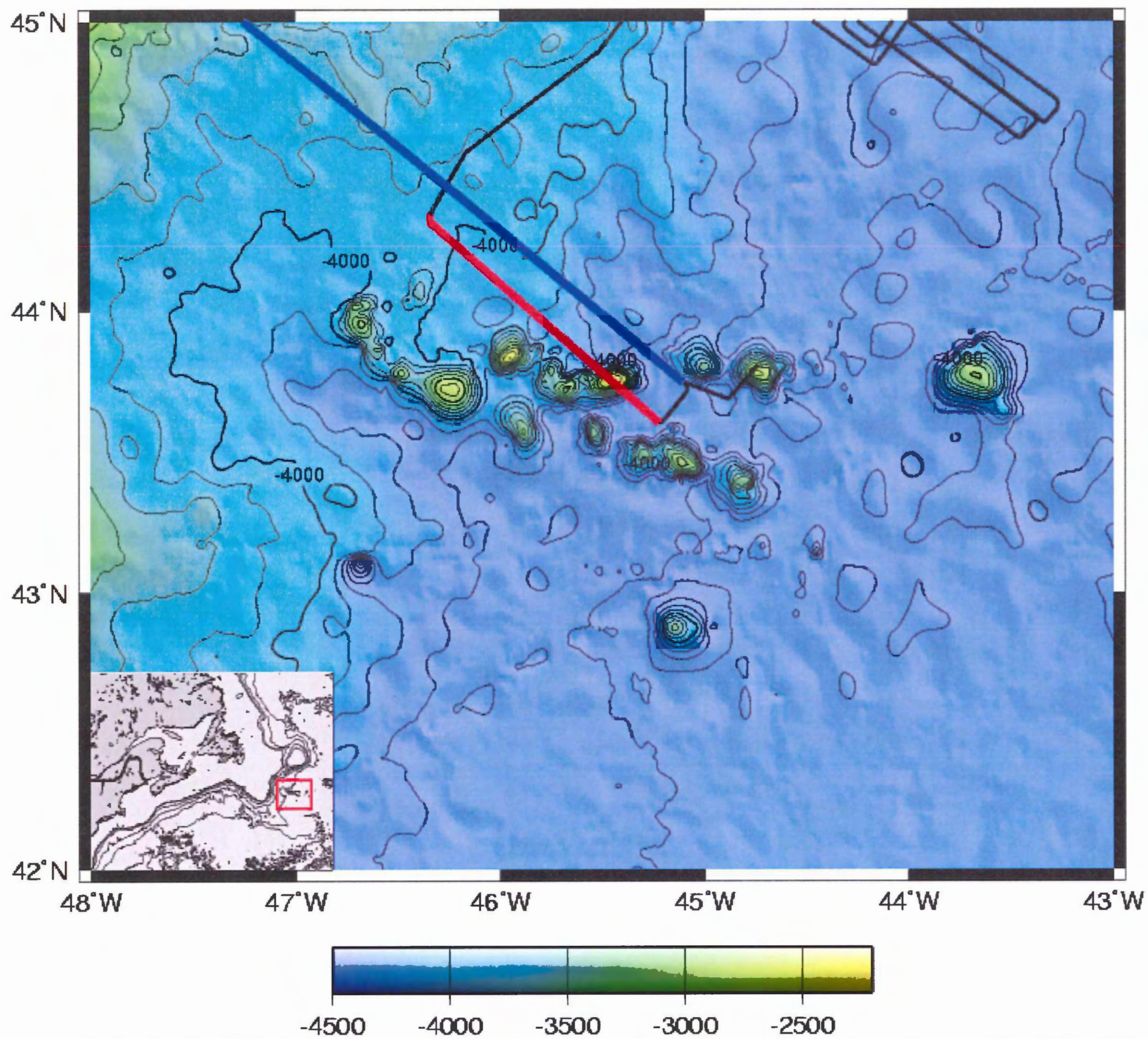

Figure 1.3.3 Detailed map of Newfoundland Seamounts in the Newfoundland Basin. Line 306, red, transects the Scruncheon seamount. Line 3mcs2 in blue and SCREECH auxiliary lines in black.

1.4 Purpose

The primary purpose of this study is to process seismic line 306, an auxiliary multichannel seismic line acquired in the Newfoundland Basin as part of the SCREECH seismic program. The final stacked migrated section will be compared to parallel line 3mcs2 (Lau personal communication, 2003) to determine if structures can be correlated between the two lines. In particular, this study will determine if two basement highs identified in the OCT on line 3mcs2 extend south to line 306.

Chapter 2: Previous Work

2.1 SCREECH Survey

The SCREECH survey collected seismic data over the Newfoundland continental margin. This program aims to identify and interpret rifting and extensional tectonic features on and around the Grand Banks, the Flemish Cap and in the Newfoundland Basin. Detailed wide-angle ocean bottom seismometer (OBS) and vertical-incidence multichannel seismic (MCS) data were acquired along three main transects across the Newfoundland margin with auxiliary MCS data parallel and crosscutting the main transects. The SCREECH data will be used to determine the origin and crustal affinity of thinned crust observed between extended continental and oceanic crust in the Ocean Continent Transition (OCT) zone.

Helen Lau processed the most southern main transect, line 3mcs2, as part of a PhD thesis at Dalhousie University. The processing sequence for line 3mcs2 formed a basis for the processing sequence of line 306. The stacked time-migrated section showed evidence of a curious structure in the seaward portion of the OCT. Processing of line 306 was completed to examine the regional extent of this structure.

2.2 Previous studies within the Newfoundland Basin

Previous studies of the OCT in the Newfoundland Basin have given rise to conflicting theories regarding the formation of the thinned crust found in this zone. Srivastava et al. (2000) propose that slow initial seafloor spreading prior to M0 of the Mesozoic spreading series formed weak magnetic spreading anomalies west of the J-anomaly in the OCT. While the velocity structure of this zone suggests the presence of serpentinized peridotite and gabbro, Srivastava et al. (2000) suggest the weak linear magnetic anomalies, which resemble seafloor anomalies, provide evidence that some basalt must be present. Previous authors (Louden and Chian,1999; Brun and Beslier, 1996) have interpreted this velocity structure to indicate the presence of serpentinized mantle suggesting the OCT formed by mantle exhumation. Tucholke et al. (1989) interpreted results from an extensive regional seismic program, concluding that the OCT represents extended continental crust. They propose fault blocks in this zone are similar in structure, size, and internal geometry to continental blocks observed on the conjugate margin. In the Central Newfoundland Basin evidence to support this theory is problematic due to reverberations of a high amplitude basin-wide reflection, the U-reflector, which closely overlies or intersects the underlying basement, masking the basement reflections, Figure 2.2.1. Tucholke et al. (1989) has followed other authors (Jansa and Wade, 1975; Tucholke and Ludwig, 1982) and interpreted the U reflector to represent a widespread unconformity coincident with the breakup of the Grand Banks from Iberia. These authors have correlated the event with the Avalon unconformity extending onto the Grand Banks. Preliminary results of 3mcs2 processing (Lau, personal communication, 2003) do not support the landward continuation of the U reflection and its merge with the Avalon unconformity. Proposed ODP drill sites in the central Newfoundland Basin in conjunction with results from the SCREECH survey aim to determine if the U reflection is a synrift unconformity, a break-up unconformity, a sedimentary event such as a turbidity flow or a basalt flow (Tucholke, 2000)

2.3 Seismic Line 3mcs2

Line 3mcs2 extends from the thick continental crust of the Grand Banks, through thinned continental crust, the OCT and into thinned ocean crust. The seismic section is presented in

Figure 2.3.1 in the back sleeve. Figure 2.3.2 shows the locations of shot points for both line 3mcs2 and line 306 relative to the bathemetry of the Newfoundland Basin.

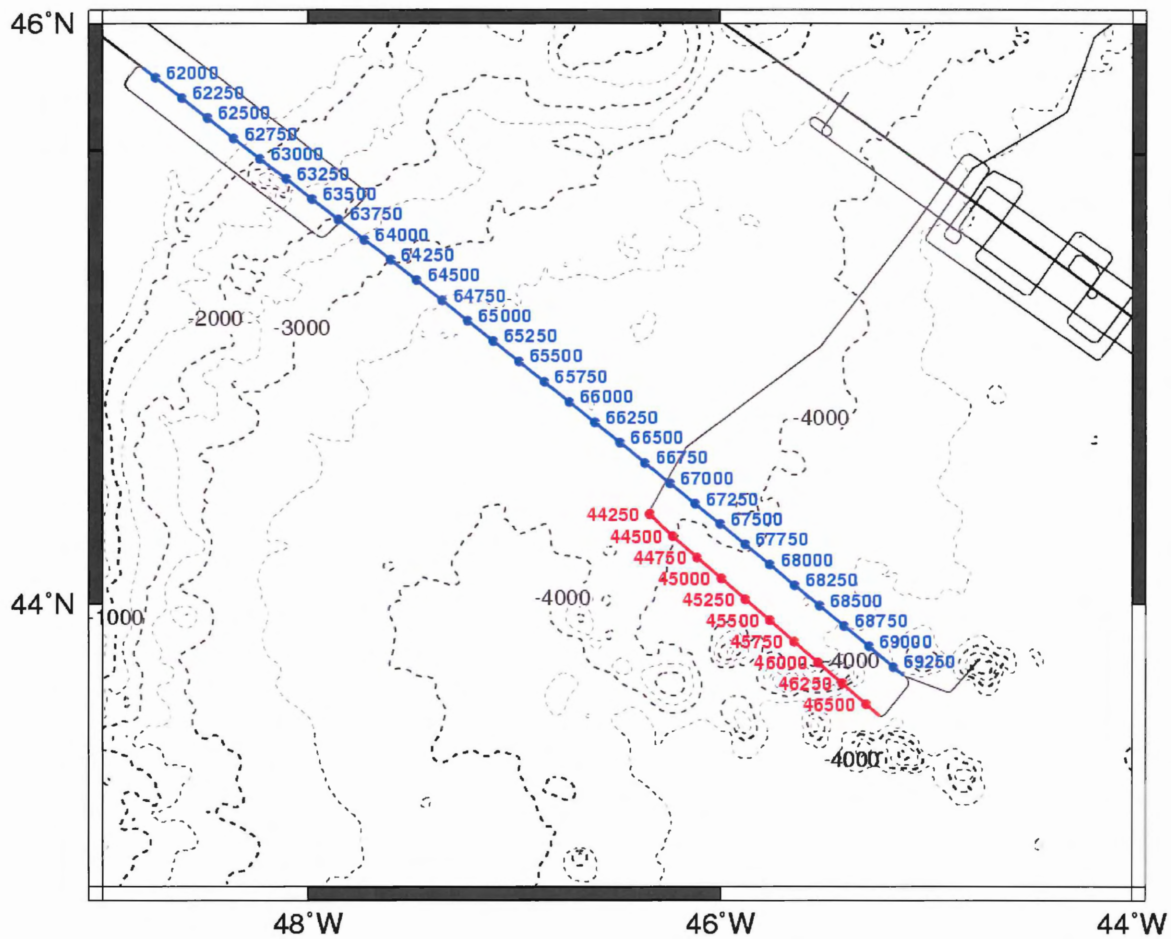

Figure 2.3.2 Line 3mcs2 and 306 with shot points labelled every 250 shots, blue and red line respectively. Auxiliary SCREECH lines in black for reference. Bathemetry contoured every 500 meters below sea level.

The continental crust is thick in the vicinity of the Grand Banks and thins seaward. Depth to the basement reflector increases as the continental crust becomes progressively thinner but remains well defined and continuous with gentle topography. A series of seaward dipping rotated fault blocks are identified within the continental crust, Figure 2.3.1. The largest landward fault block is followed by smaller blocks which become progressively obscure and difficult

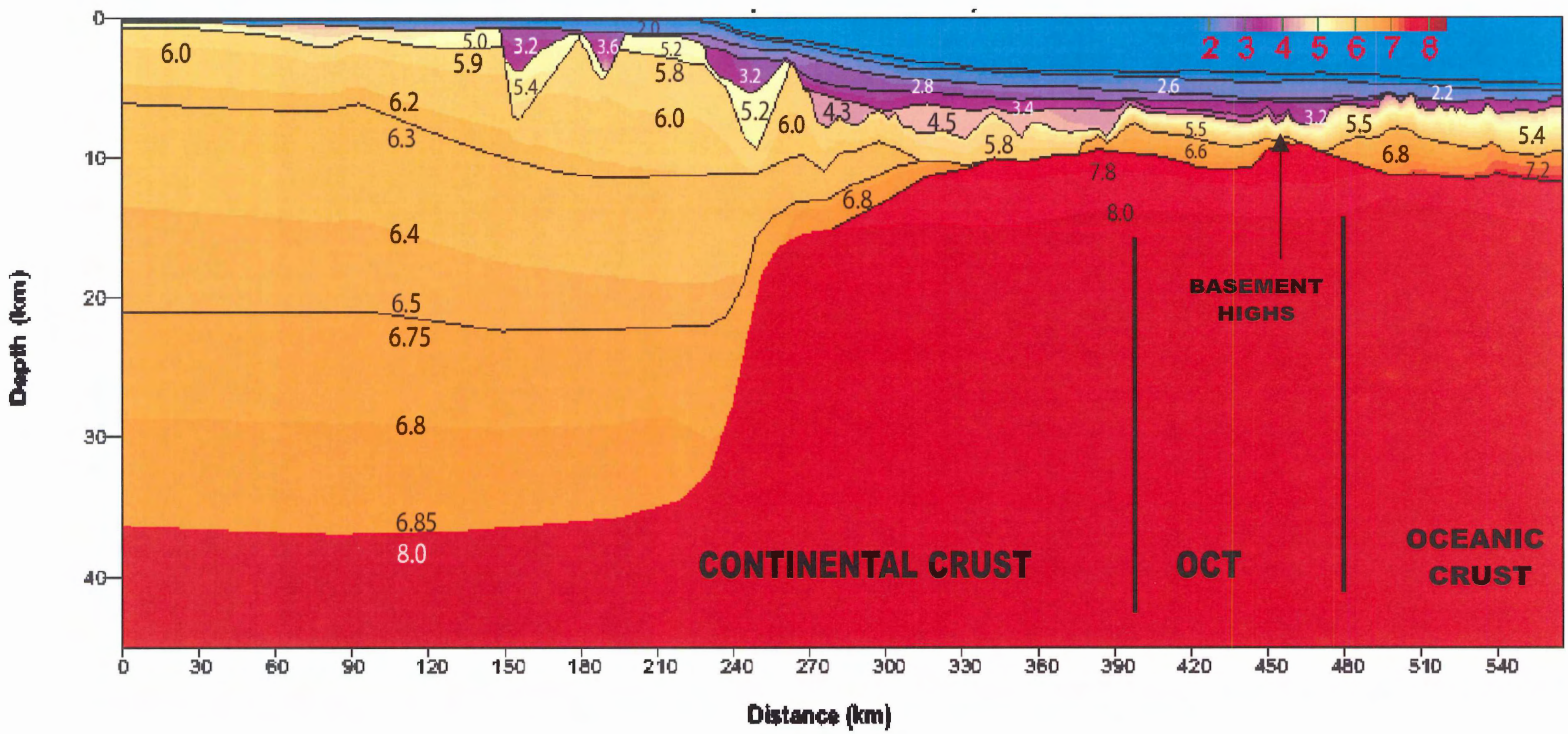

Figure 2.3.3 Velocity model for line 3mcs2 with depth on the y-axis and distance on the x-axis. Velocities in km/s. Approximate locations of continental crust, the OCT and oceanic crust (Lau, 2003).

to distinguish oceanward. Continuous internal reflections and a velocity of 6.0 km/s, Figure 2.3.3, characterize the continental crust.

At approximately shot 65400 the seismic character of the crust changes, becoming flatter and losing internal reflectors. The topographic high at shot 66100 marks the termination of rifted continental crust and the onset of the OCT. In the OCT the basement becomes flat with little topography. The overlying U reflector masks the reflection from the top of the basement making it difficult to distinguish. There are no distinguishable internal crustal reflectors in this portion of the OCT. A below average mantle velocity of 6.6 km/s is modeled for crust beneath the basement, Figure 2.3.3, which is interpreted to represent serpentinized mantle exhumed during the late stages of rifting.

Two basement highs at shots 67100 and 67275 exhibit numerous internal crustal reflections, Figure 2.3.1. These highs resemble the continental fault blocks present in the thinned and brittlely deformed continental crust. Although the velocity model is difficult to constrain over such a small area, the velocities are indicative of continental crust, Figure 2.3.3. It is tempting to consider these features to be of continental origin, but their large displacement seaward of the defined continental crust blocks complicates such an interpretation.

A ridge coinciding with the position of the J-anomaly lies between shots 68050 and 68250. The top of the basement is a high frequency reflector with intense hyperbolic reflectivity produced by uneven topography which is characteristic of oceanic basement. As expected, there are no internal reflectors from the ocean crust. Velocities of 5.4 km/s have been modeled for the oceanic crust, Figure 2.3.3.

Chapter 3: Data acquisition and seismic processing sequence: Line 306

3.1 Acquisition Parameters

R/V Ewing recorded the MCS data with its 480-channel, 6 km long Syntron streamer with hydrophone group spacings of 12.5 m, Figure 3.1.1(a). A sample rate of 4 ms was used because little energy was expected above the 4-ms Nyquist frequency of 125 Hz and later spectral analysis of the data showed a sharp drop-off above 80 Hz (Tucholke and Holbrook, 2000). Shooting was done on distance with a principle shot interval of 50 m. Shots were fired with R/V Ewing's 20 gun, 8540 cubic inch (131 litre) airgun array with gun sizes ranging from 145 cubic inches to 875 cubic inches, Figure 3.1.1(b). Guns were towed at a nominal depth of 7.5 m, though the guns were often above this depth when ship speed increased.

3.2 Seismic processing sequence

The seismic processing sequence for line 306 is based on the processing sequence for the oceanward portion of seismic line 3mcs2 (Lau, personal communication, 2003). The GLOBE Claritas software package was used for processing. GLOBE Claritas is an interactive software package for processing 2D and 3D seismic data with ongoing developments that began in mid '80s by the Institute of Geological and Nuclear Sciences, an independent New Zealand government-owned science organization (Ravens, 2001).

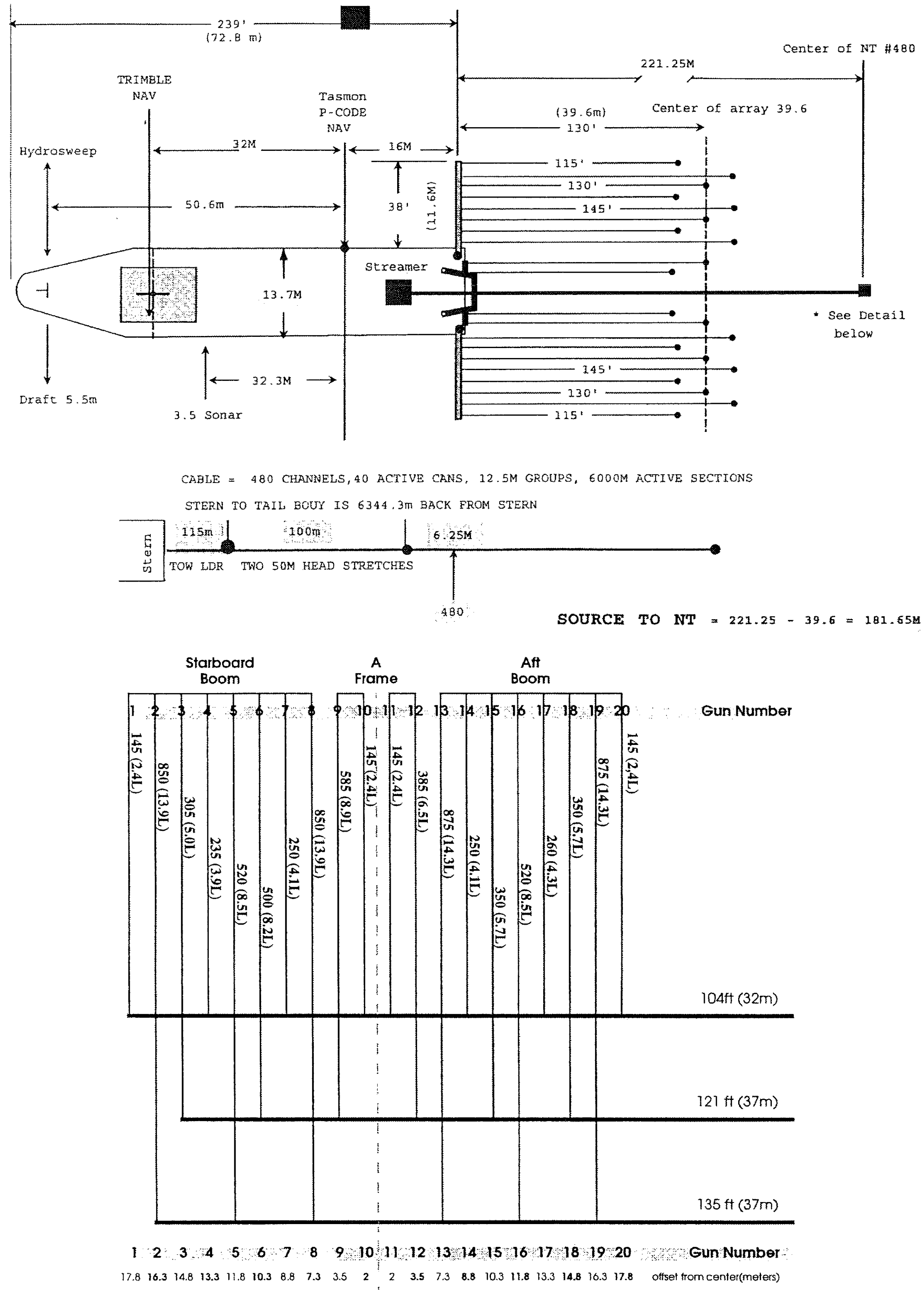

Figure 3.1.1 Acquisition parameters and geometrical configuration of the streamer, (a), and the array of the 20 air gun source, (b), onboard R/V Maurice Ewing. Modified after Tucholke and Holbrook (2000).

3.2.1 SEG Y Standard Data Exchange Format

Raw data were recorded on magnetic tapes aboard the Maurice Ewing in the Society of Exploration Geophysicists Y (SEG Y) format. As part of this study's processing sequence the segmented SEG Y data from the tapes were read into the GLOBE Claritas seismic processing software and saved as one large Claritas data disk file.

SEG Y is a standard data exchange format adopted in the mid 1970's because of the growing need to standardize an acceptable data exchange format (Barry et al., 1975). The widespread use of SEG Y data has produced many variations of the SEG Y format and numerous revisions of the standard by the SEG Technical Standards Committee (Norris and Faichney, 2002). The basic components of the SEG Y file structure can be divided into 3 components; the reel header, binary header and the seismic traces. The reel header, sometimes referred to as a textural header (Norris and Faichney, 2002), contains 40, 80 byte lines of text describing the seismic data in the SEG Y file (Cohen and Stockwell, 2002). The second component of the SEG Y file is a 400 byte binary header. The binary header contains information that affects the entire SEG Y file such as the sampling rate, trace length and the data sample format code (Barry et al., 1975). The last part of the SEG Y file format are the seismic data traces each proceeded by a trace header. The trace headers contain trace attributes such as shot, shot number, and offset in the first 180 bytes (Norris and Faichney, 2002). Bytes 180-240 are reserved for optional information (Barry et al., 1975) and are assigned in the GLOBE Claritas software to variables required for the different processors (Ravens, 2001).

3.2.2 Geometry and CMP

Geometry was configured for all of line 306 using the geometry of the streamer and shots to calculate the locations of the common midpoints (CMP). CMP refers to the point on the surface shared by numerous source-receiver pairs halfway between the source and receiver. Seismic traces that belong to the same CMP are grouped together in a CMP gather. The number of traces per CMP gather defines the fold of the survey. This redundancy among source-receiver pairs enhances the quality of the seismic data when the traces are stacked.

For seismic line 306 the streamer was 6 km long with a spacing of 12.5 meters between the 480 receivers and the shot spacing was 50 m. This equates to a CMP spacing of 6.25 m with a nominal fold of 60. The linearity of the survey created a simple geometry that only became complex on the most northern portion of the line where the ship turned on a 45 ° angle. Initial attempts to assign the geometry used GLOBE Claritas's 3 dimensional geometry processor which required a shot file, with shots and locations, and a streamer file, which contained the near and far offsets of the receivers in the streamer. When CMPs were assigned using this method the fold fluctuated between 50 and 70. Traces were not assigned to the proper CMP and often traces were excluded from their proper CMP. This is obviously a flaw in the Claritas software since later work discovered a geometry processor for marine surveys, which assigned traces to their proper CMPs.

The only persisting problem was in the area where the ship turned. This occurred because theoretically, traces common to one CMP represent reflections from the same subsurface location. This assumption becomes invalid when the streamer does not follow behind the ship in a straight line, a phenomenon known as feathering of the streamer. Feathering becomes a major problem when significant ocean currents are present or when the ship turns.

Once the CMP numbers were assigned to the various traces the traces were sorted by CMP. Problems were again encountered with the sorting processor, which could not handle shots with more than 200 traces. Once the processor was fixed remotely by Claritas support the traces were sorted to CMP. Zero traces were added for missing shots 45288 and 45292-45299 because the sorting processor could not handle missing traces. These traces were subsequently removed prior to further processing.

3.2.3 Bandpass Filtering

A 7-10-70-85 bandpass filter was applied to the CMP gathers, which was the filter chosen for line 3mcs2. Variations of this filter with both larger and smaller highpass and lowpass frequencies were applied with little variation in the filtered result. The 7-10-70-85 bandpass filter was chosen for consistency upon comparison to 3mcs2. The bandpass filter allows frequencies within the specified range to pass without attenuation by the filter. The gradient on either side of the bandwidth prevents spiking of the filtered signal. This particular filter is designed to filter out the low frequency and high frequency noise without altering the signal from reflections. The most noticeable effect from filtering was the removal of low frequency noise that persisted throughout the section.

3.2.4 Velocity analysis

Velocity analysis were performed on every 200th CMP except in areas of complex structure which were analysed every 50th CMP. Various methods for velocity analysis exist but all determine normal moveout (NMO) velocities which are then applied to the CMP gathers.

NMO velocities are determined using the Pythagorean Theorem and the travel time equation. The travel time equation as a function of offset is:

$$t^2(0) = t^2(x) + \frac{x^2}{v^2} \quad (3.1)$$

where x is the offset between the source and receiver positions, v is the velocity of the medium above the reflecting interface, and *t(0)* is the two-way travel time of the normal incidence reflection. Once the normal moveout velocity is estimated the travel times can be corrected to remove the influence of offset. The normal moveout correction is the difference between *t(x)* and *t(0)*:

$$\Delta t_{NMO} = t(x) - t(0) \quad (3.2)$$

Semblance was used as a first pass velocity determination for the brute stack. Semblance determines NMO velocities that correspond to the best coherency of the seismic signal along a hyperbolic trajectory over the entire spread length of the CMP gathers (Yilmaz, 1987). Coherence is a measure of the degree of fit of a theoretically derived hyperbolic curve at a given travel time for a chosen NMO velocity. Various types of coherency measure can be used as attributes in computing velocity spectra with semblance the most common. Semblance is a measure of the coherence of the stacking process; when it equals 1 it implies perfect selection of the normal moveout correction. To obtain semblance values incremented NMO velocities are applied to a CMP gather and the coherency of each velocity application is contoured on a plot of velocity on the x-axis versus two way travel time on the y-axis, Figure 3.2.1. The initial stacking velocities were chosen for every 50th CMP from the semblance plots. The constant velocity gather and constant velocity stack proved these velocity picks were only accurate in the shallow sediments.

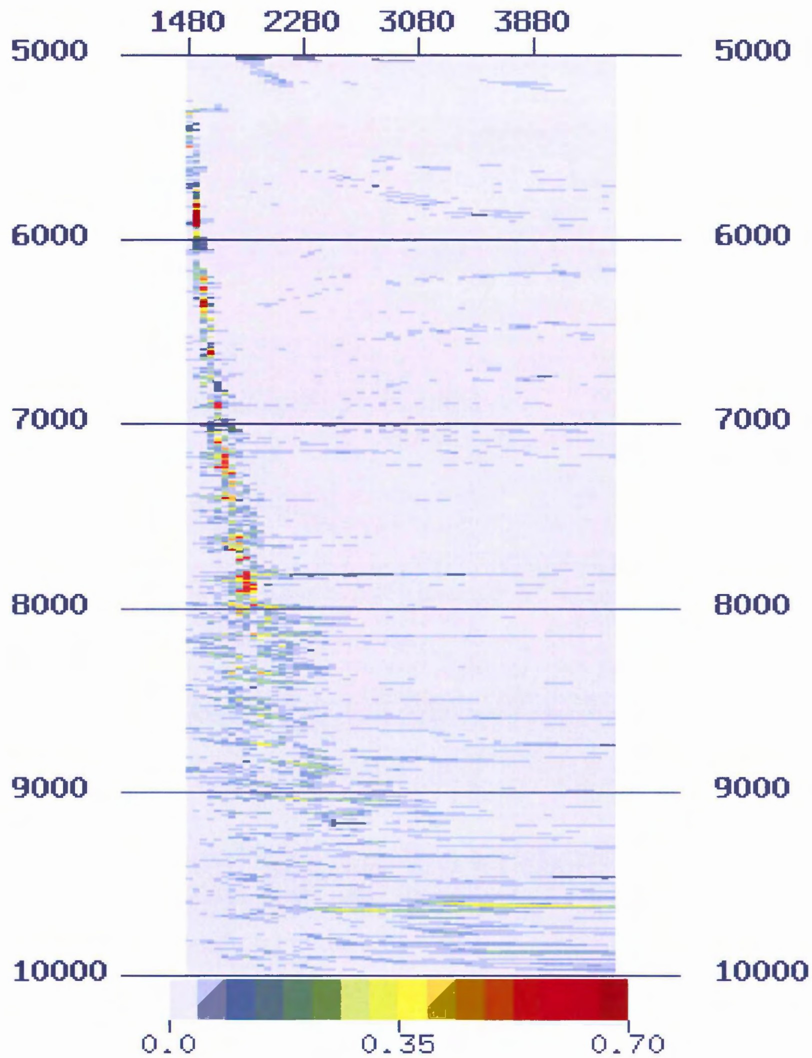

Figure 3.2.1 Semblance, coherence contoured velocity plot with two-way travel time in ms on the y-axis and velocity in m/ms on the x-axis. The colour bar measures coherence from 0 to 0.7. A coherence of 0.7, red, implies the best stacking velocity. The trend of high coherence is present until 8000 ms after which velocity picks are more obscure.

Constant velocity gathers and constant velocity stacks provided a more detailed velocity determination for the final stack. For the constant velocity gather a CMP gather is repeatedly

NMO corrected using a range of constant velocities with the results displayed in a panel for comparison. Data are overcorrected, upturned, at low velocities and undercorrected, downturned, at higher velocities. The best stacking velocities are obtained when a particular horizon is flat, Figure 3.2.2. Velocities that flatten individual horizons are picked to build up a velocity function for the particular CMP. The constant velocity stack applies a range of constant velocities and stacks specified CMP gathers. Velocities that result in high amplitude, continuous reflectors provide the best stacking velocities.

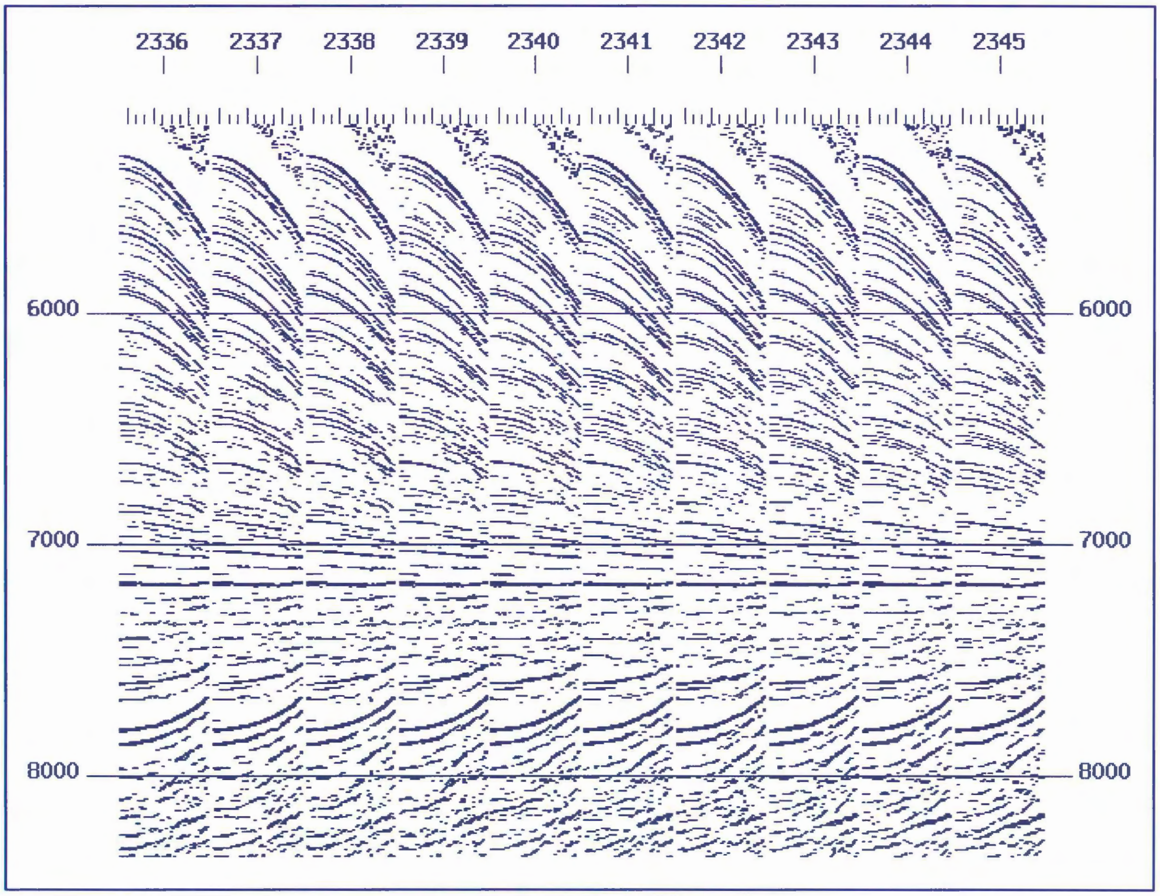

Figure 3.2.2 GLOBE Claritas constant velocity gather with a velocity of 1725 m/ms applied to 10 CMP gathers, CMP 2336-2345. The reflector at 7200ms, two-way travel time, is flat while reflectors above are downturned, over corrected, and reflectors below are upturned, under corrected.

Velocity picks were both obvious and consistent within the sediment package. Once the basement was reached velocities were often difficult to distinguish from peg legs of the overlying sediments. Determination of crustal velocities was difficult because of the lack of coherent reflectors. Therefore, the velocity analysis and subsequent time-migrated section focus on distinguishing the basement reflector. Velocities for the basement were even less obvious with the onset of oceanic crust because of the increased topography and intense hyperbolic reflectivity. Velocity analysis was also challenging in the vicinity of the seamount, again, due to the interference from diffractions.

3.2.5 Stack

The Claritas NMO processor applied the output velocity model from the velocity analysis to the CMP gathers. Traces within one CMP were summed or stacked together. Noise was diminished and reflection signals enhanced. The Claritas NMO processor assumes the classic Pythagoras equation linking the recorded time with the corrected time and the offset distance divided by the velocity (Ravens, 2001).

As a result of the normal moveout correction a frequency distortion occurs for shallow events at large offsets. The dominant period of the waveform is stretched creating a period after NMO corrections that is greater than the original period. This phenomenon, known as stretching, is a frequency distortion that shifts events to lower frequencies. Stretching can be quantified as:

$$\frac{\Delta f}{f} = \frac{\Delta t_{NMO}}{t(0)} \qquad (3.3)$$

where f is the dominant frequency, Δf is the change in frequency and Δt_{NMO} is given by equation (3.2). In Claritas a stretch mute defines the percentage stretch above which to mute the trace. For 1ms sampled data a 30% stretch mute will zero samples between 0.7 and 1.3 ms. The taper length defines the length of the linear taper, in ms, over which the stretch mute is applied (Ravens, 2001). The smaller the stretch mute value the larger its effect is on the traces.

Velocity analysis determines stacking velocities or NMO velocities approximately equivalent to the root mean square, RMS, velocities. The RMS velocity down to a reflector is defined as:

$$v_{rms}^2 = \frac{1}{t(0)} \sum_{i=1}^{N} v_i^2 \Delta t_i(0) \tag{3.4}$$

where Δt_i is the vertical two way travel time at a velocity v_i through the i-th layer. By making the small-spread approximation, offset is small compared to the depth, the series in (3.4) can be truncated to produce:

$$t^2 = t^2(x) = t^2(0) + \frac{x^2}{v_{rms}^2} \tag{3.5}$$

Comparison of (3.1) and (3.5) show the RMS and NMO velocities are equal at small offsets. At large offsets this approximation is not valid; therefore, multilayered sections with arbitrary dips are approximated with a small-spread hyperbola (Yilmaz, 1987).

3.2.6 Migration

Events on a stacked unmigrated section are often not in their true subsurface locations creating an incoherent and discontinuous seismic section that does not show the true subsurface geometry. During seismic acquisition signals returning from subsurface reflectors are plotted directly below the recording geophone. Although this does not pose a problem for flat lying strata, dipping reflectors and complex structures whose normal reflections arrive at an angle to the geophone are shifted down-dip and increased in length. Prior to migration incoherent reflectors are often replaced by large diffraction hyperbolas. Migration addresses this problem by restoring geometrical relationships between seismic events on a time section to make the stacked section appear similar to the geologic cross section along the seismic line. Migration resolves structural complexities and dipping interfaces, collapses diffraction hyperbola and delineates detailed subsurface features such as fault planes.

The basic theory of seismic migration is described in Figure 3.2.3. The reflections from a dipping interface C' D' are recorded on surface geophones A and B. On the seismic record these reflections are plotted directly below geophones A and B at the subsurface locations C and D. Migration moves C-D to its correct position, C'-D', which decreases the length of the reflector and moves the reflector updip increasing the gradient from è$_t$ to è$_T$.

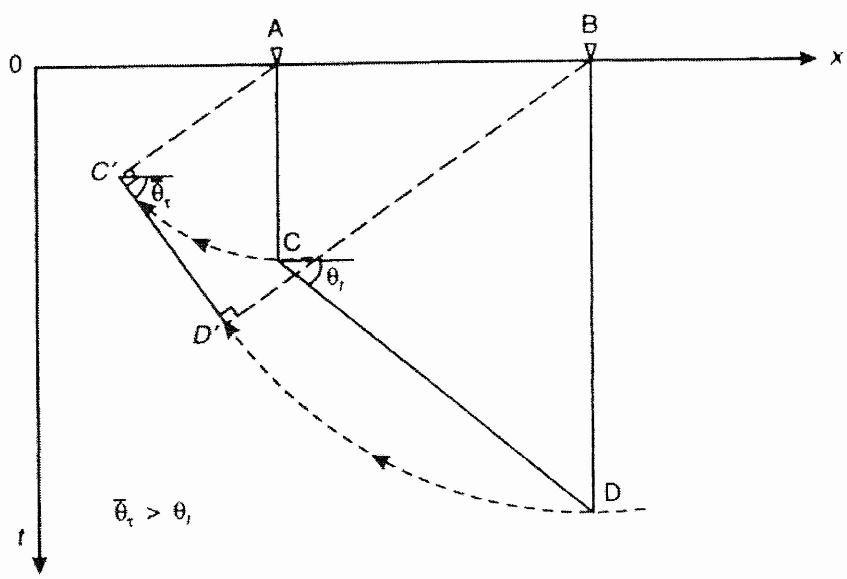

Figure 3.2.3 Principle of seismic migration. The dipping reflector C-D on a stacked section is moved to its correct geometry C'-D' on the migrated section. Modified after

The Claritas FDMIG processor, a steep dip finite difference migration scheme, was chosen for migration because it allows both vertical and lateral velocity variations. A conversion program in Claritas quickly converted RMS velocities to interval velocities creating a scaled velocity model suitable for application in the FDMIG processor. Interval velocity, the velocity of a particular layer, is calculated from the RMS velocity by the Dix Equation:

$$v_{layer} = \sqrt{\frac{(v_{rms.B}^2 t_n - v_{rms.T}^2 t_n)}{(t_B - t_T)}} \qquad (3.6)$$

where t_B and t_T are the two way travel times to the top and base reflectors.

The Claritas program that converted RMS velocities to interval velocities did not accurately calculate interval velocities for much of the basement in the vicinity of both the oceanic crust and seamount. Inaccurate interval velocities, which overmigrated the water bottom reflection, were a persistent problem. As a result, many of the migration velocities had to be modified within the velocity file on a trial and error basis. The velocity file was easily modified and the finite difference migration repeated on the problematic sections until the majority of diffractions were collapsed. Aside from the inaccuracy of the interval velocities, the finite difference migration did a very good job of collapsing diffractions and delineating dipping reflectors.

Chapter 4: Results

4.1 Output from processing sequence

The final stacked and migrated version of line 306 is presented in Figure 4.1(a). Only 10 of the total 16.38 seconds of recorded two-way travel time are displayed. Velocity analyses were not performed for deeper crustal reflectors but instead, focused on determining the velocities for the basement and overlying sediment in the first 10 seconds of the record. The two-way time to basement averaged 8 seconds while velocity analyses were preformed to an average time of 9 seconds. In the vicinity of the seamount velocity analyses were only applied to the first 0.5 seconds beneath the water bottom reflection because internal reflections were not present.

The direct arrivals and noise above the water bottom reflection were not muted out. This noise is visible in the upper portion of the section. Artifacts from the migration are evident at the beginning and end of the section. The large diffractions are caused by the reflection of events back into the section, Figure 4.1. This occurs because migration moves events past the edge of the section but the zero amplitude or zero gradient boundary assumptions of the finite difference migration algorithm (Yilmaz, 1987) does not allow the reflections to move off the section. The events are then forced to reflect back into the section.

Large diffractions are also visible around the seamount, Figure 4.1, which persisted through stacking and migration. The interpolation between velocity picks for the western flank of the seamount in the migration velocity file is curious. It appears that the interpolation moves up then jumps over, rather than following a linear trend as it moves up the flank of the seamount, Figure 4.2. This bulging effect has resulted in overmigration on the flanks of the seamount. The change in slope from the steep flank to flat top of the seamount is characterized by large diffractions. The large diffractions at the top of the seamount are a result of overmigration.

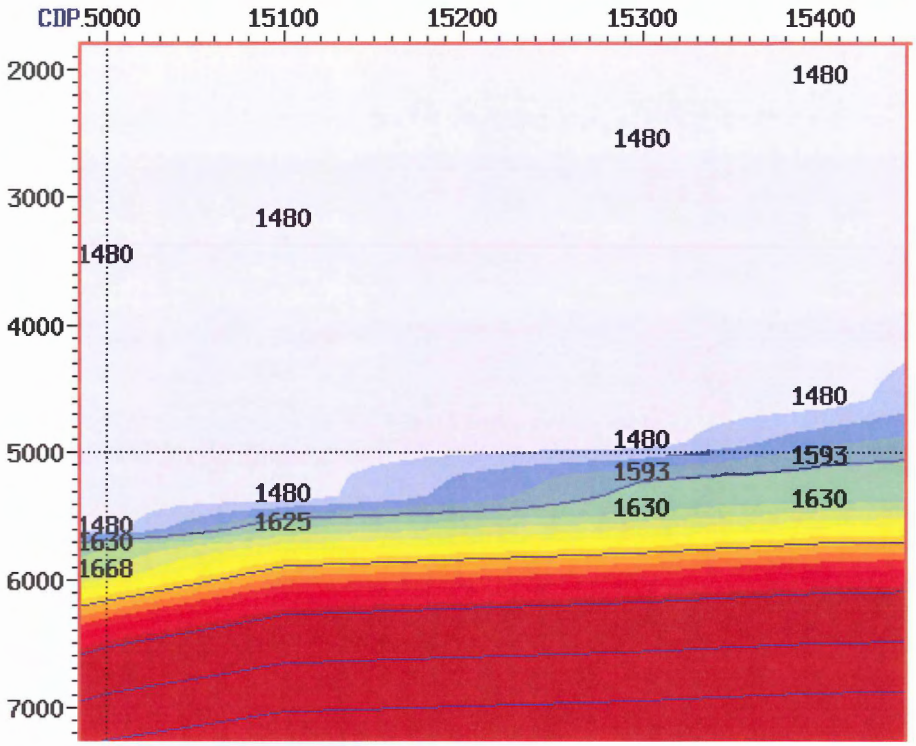

Figure 4.2 Velocity model on the western flank of the seamount showing the nonlinear interpolation between adjacent velocity picks. This effect resulted in overmigration along the flanks of the seamount. Velocity picks are displayed in m/s. Two-way travel time is labelled on the y-axis in ms and CDP number on the x-axis.

Attempts were made to eliminate these diffractions. They were significantly reduced by lowering the interval velocities, but they could not be entirely removed. A large water bottom multiple is present at 7 s two way travel time below the seamount.

Small diffractions remain within the sediment on the first 1000 CMPs. The turn at the start of line 306, and subsequent feathering of the streamer, smeared the CMP locations. Stacking velocities and the subsequent calculated interval velocities in this area were not accurate. This portion of the line was retained to allow for visual comparison to line 3mcs2.

Chapter 5: Discussion

5.1 Seismic Line 306

The stacked migrated version of line 306 is presented in Figure 4.1(a) along with a portion of line 3mcs2 for comparison and correlation purposes, Figure 4.1(b). Line 306 corresponds to the section east of shot 67000 on line 3mcs2. The U-reflector identified on line 3mcs2 is present from shot 44210 to 44325 on line 306. This portion of line 3mcs2 corresponds to the turn on line 306. Normally, the shots occurring within the turn on line 306 would have been removed from the data set due to the smearing of the CMPs but omission of this data, which contains the only reflections on line 306 from the U-reflector and OCT, would make it difficult to correlate the two seismic lines.

The U reflector is present at the beginning of line 306 and terminates against a wide basement high at shot 44350. This basement high is interpreted as a rotated fault block of uncertain crustal affinity. This block is distinguished from crust of the OCT to the west which is smooth with little basement topography, and from basement to the east which has hyperbolic reflectivity and uneven basement topography identifying it as oceanic crust. This high is also similar to fault blocks in the thinned, brittley deformed continental crust on line 3mcs2, Figure 2.2.1. Internal reflections are visible but it is unclear if they represent real reflections or are peglegs from the overlying sediment. Between this block and the adjacent ocean crust there is a thick sequence of highly reflective sediments which mask the basement reflection. A steep east dipping reflector below this sediment package could represent a basement reflection or an internal reflection indicative of either a compositional variation or a fault plane.

The single basement high or fault block on line 306 can be correlated with the seaward basement at shot 67275 on line 3mcs2. Line 306 does not extend landward enough to image the second basement high on line 3mcs2. Although the single basement high on line 306 is deeper in the section and bounded by a thicker sequence of sediments than the 2 highs on line 3mcs2, it is not characteristic of either the OCT or oceanic crust. The continuity of the structures between lines 306 and 3mcs2, Figure 5.2, approximately 20 km apart, implies that the structures found on line 3mcs2 represent a significant tectonic feature. These structures could represent continental crust that drifted into the OCT during the late stages of rifting, a phenomenon not documented on any other continental margin. The blocks are more likely tectonized oceanic crust that formed in the early stages of slow seafloor spreading around M0 time (Srivastava et al., 2000: Srivastava and Keen, 1995). Basalt that formed at the spreading center would have cooled while extension continued resulting in brittle deformation. The internal crustal reflections apparent on lines 306 and 3mcs2 would then represent normal faults.

The rest of line 306 is quite similar to line 3mcs2, with the exception of the Scruncheon Seamount found on line 306. The basement is smooth, flat and continuous east of the fault blocks until shot 45100 at the onset of the J-anomaly ridge. After the crest of the J-anomaly ridge, time to basement increases and the resolution of the basement reflection decreases with intense diffraction hyperbolas, only some of which were collapsed by the migration process. Refinements of interval velocities in this section will collapse more diffraction hyperbola and create a more coherent basement reflection. Basement begins to rise again near the Scruncheon seamount at shot number 46000. In the area of the largest gradients, on the flanks of the seamount, the basement reflector is not well defined. Oceanic crust continues east of the seamount.

Sediment thickness is constant along the line decreasing at the J-anomaly Ridge and terminating against the seamount. Two deep troughs in the surface of the sediment are present at the western base of the seamount. Sediment is thin and difficult to distinguish on top of the seamount. The sediment package is substantially thinner and different in character on the eastern side of the seamount.

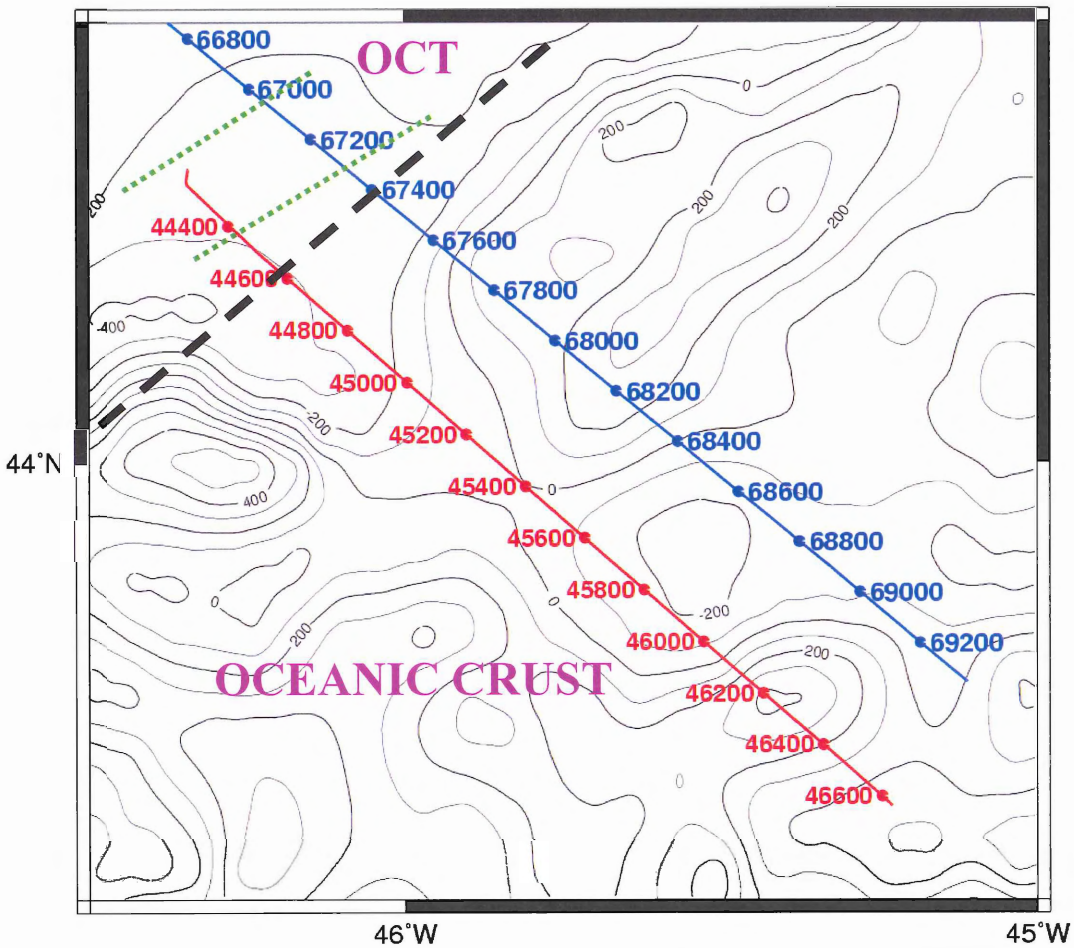

Figure 5.2 Continuity of structures between lines 306, red, and 3mcs2, blue. Green dotted lines connect the basement highs in the OCT on the two lines. Dotted black line is the inferred boundary between the OCT and Oceanic crust. Magnetic contours every 100 nT. The J-anomaly ridge is the NE trending high, through the two lines.

Chapter 6: Conclusions

6.1 Conclusions

SCREECH line 306 within the Newfoundland Basin was processed with the GLOBE Claritas seismic processing software. The velocity analysis determined stacking velocities for the sediment, basement and upper crustal reflectors. The final stacked, migrated section was compared to adjacent SCREECH line 3mcs2. The fault block at the edge of the Ocean Continent Transition (OCT) on line 306 correlates with two similar fault blocks on line 3mcs2, marking the termination of the OCT and the onset of oceanic crust. The continuity of these structures between line 306 and 3mcs2 suggests they represent a significant tectonic feature. Increased resolution of the basement around this fault block and detailed velocity analyses of the underlying crust are recommended in order to help constrain the mechanism for formation of these fault blocks.

6.2 Recommendations for Future Work

Time constraints prevented application of the full processing stream to line 306. Further processing of line 306 including deconvolution, multiple suppression, velocity analysis on deep crustal reflections including determination of the MOHO reflection are recommended. Deconvolution would determine if the reflections below the single basement high are crustal reflections or peglegs of the overlying U-reflector. Integration of the results from seismic processing of line 306 with the results from the other SCREECH lines and from the proposed ODP drilling north of this study could confirm the crustal affinity of the OCT and confirm the proposed boundary of the OCT.

References

Barry, K.M., Cavers, D.A. and Kneale, C.W., 1975. Recommended Standards for Digital Tape Formats. *Geophysics*, **40**, no. 02, 344-352.

Cohen, J. K. and Stockwell, Jr. J. W., 2002. CWP/SU: Seismic Unix Release 36: a free package for seismic research and processing, Center for Wave Phenomena, Colorado School of

Grant, A.C. and McAlpine, 1990. The continental margin around Newfoundland, in Geology of the continental margin of Eastern Canada, M.J. Keen and G.L. Williams eds., Geology of Canada no. 2 Geological society of Canada, 239-293.

Jansa, L.F. and Wade, J.A., 1975. Geology of the continental margin off Nova Scotia and Newfoundland, in W.J.M. van der Linden and J.A. Wade, eds., Offshore geology of Eastern Canada, **2**, Regional geology: Geological Survey of Canada Paper 74-30, 51-105.

Lau, H. Personal Communication, 2003. PhD research.

Louden, K. E. and Chian, D. 1999. The deep structure of non-volcanic rifted continental Margins, *Phil. Trans. Royal Society of London A* **357**, 767-804.

Masson, D.G. and Miles, P.R., 1984. Mesozoic seafloor spreading between Iberia, Europe and North America, *Marine Geology*, **56**, 279-287.

Norris, M.W. and Faichney, A.K., 2002. SEG R rev 1 Data Exchange Format. SEG Technical Standards Committee, Society of Exploration Geophysicist (unpublished), 46 p.

Rabinowitz, P.D.,, Cande, S.C. and Hayes, D.E., 1978. Grand Banks and J-Anomaly Ridge, *Science*, **202**, 71-73.

Ravens, J., 2001. Globe Claritas, Seismic Processing Dictionary: 3rd edition.

Reid, I.D., 1994. Crustal tructure of a nonvolcanic rifted margin east of Newfoundland, *Journal of Geophysical Research*, **99**, 15,161-15,180.

Reynolds, J.M., 1998. An introduction to Applied and Environmental Geophysics: Wiley, Toronto

Sullivan, K.D. 1977. The structure and evolution of the Newfoundland Basin, Offshore Eastern Canada. Ph.D. Thesis, Dalhousie University, Halifax Nova Scotia, 294 pp.

Sullivan, K.D. and Keen, C.E. 1977. Newfoundland Seamounts: Petrology and Geochemistry; in: Volcanic Regimes of Canada,. Baragar, W.R.A, Coleman, L.C. and Hall, J.M., Geological Association of Canada, Special Paper 16, 461-476.

Sullivan, K.D. and Keen, C.E., 1978. On the nature of the crust in the vicinity of the southeast Newfoundland Ridge, *Canadian Journal of Earth Sciences*, **15**, 1462-1471.

Sullivan, K.D., 1983. The Newfoundland Basin: ocean-continent boundary and Mesozoic seafloor spreading history, *Earth and Planetary Science Letters*, **62**, 321-339.

Srivastava, S.P., Sibuet, J.C., Cande, S., Roset, W.R. and Reid, I.D., 2000. Magnetic evidence for slow seafloor spreading during the formation of the Newfoundland and Iberian margins, *Earth and Planetary Science Letters*, **182**, 61-76.

Srivastava, S.P. and Keen, C.E., 1995. A deep reflection profile across the extinct Mid-Labrador Sea spreading center, *Tectonics*, **14**, 372-389.

Tucholke, B.E. and Ludwig, W.J., 1982. Structure and Origin of the J Anomaly Ridge, Western North Atlantic Ocean, *Journal of Geophysical Research*, **87**, 9389-9407.

Tucholke, B.E., Austin, J.A. Jr. and Uchupi, E., 1989. Crustal Structureand Rift-Drift Evolution of the Newfoundland Basin; in Extensional Tectonics and Statigraphy of the North Atlantic Margins. Edited by A.J. Tankard and H.R. Balkwill, AAPG Memoir 46 247-263.

Tucholke, B. E. et al 2000 Drilling the Newfoundland half of the Newfoundland-Iberia transect: the first conjugate margin drilling in a non-volcanic rift. *ODP Drilling Proposal*

Tucholke, B. E. & Holbrook, W. S. 2000 SCREECH: Study of Continental Rifting and Extension on the Eastern Canadian sHelf. Cruise Report EW-0007 R/V Maurice Ewing.

Yilmaz, O., 1987. Seismic Data Processing: Society of Exploration Geophysicists, Tulsa.